A Chelating Cellulose Adsorbent for the Removal of Cu(II) from Aqueous Solutions

D. W. O'Connell,[1,2] C. Birkinshaw,[2,3] T. F. O'Dwyer[1,2]

[1]*Chemical and Environmental Science Department, University of Limerick, Ireland*
[2]*Materials & Surface Science Institute, University of Limerick, Ireland*
[3]*Materials Science & Technology Department, University of Limerick, Ireland*

Received 1 June 2005; accepted 7 July 2005
Published online 27 December 2005 in Wiley InterScience (www.interscience.wiley.com).
DOI 10.1002/app.22568

ABSTRACT: Regenerated cellulose wood pulp was grafted with the vinyl monomer glycidyl methacrylate (GMA) using ceric ammonium nitrate as initiator and was further fuctionalised with imidazole to produce a novel adsorbent material, cellulose-*g*-GMA-imidazole. All cellulose, grafted cellulose and functionalized cellulose grafts were physically and chemically characterized using a number of analytical techniques, including elemental analysis, Fourier transform infrared spectroscopy, thermogravimetric analysis, differential thermal analysis, and scanning electron microscopy. The cellulose-*g*-GMA material was found to contain 1.75 mmol g^{-1} epoxy groups. These epoxy groups permitted introduction of metal binding functionality to produce the cellulose-*g*-GMA-imidazole final product. Following characterization, a series of adsorption studies were carried out on the cellulose-*g*-GMA-imidazole to assess its capacity in the removal of Cu^{2+} ions from solution. Cellulose-*g*-GMA-imidazole sorbent showed an uptake of ~70 mg g^{-1} of copper from aqueous solution. The adsorption process is best described by the Langmuir model of adsorption, and the thermodynamics of the process suggest that the binding process is mildly exothermic. The kinetics of the adsorption process indicated that copper uptake occurred within 30 min and that pseudo-second-order kinetics best describe the overall process. © 2005 Wiley Periodicals, Inc. J Appl Polym Sci 99: 2888–2897, 2006

Key words: fibers; functionalization of polymers; adsorption; copper; wastewater

INTRODUCTION

Copper has become one of the most widely used metals. Specifically, it is used or produced in the manufacture of printed circuit boards, metal finishing industries, tannery operations, chemical manufacturing, and mining drainage. The properties of copper, which make it suitable for these applications, include high electrical and thermal conductivity, good corrosion resistance, ease of fabrication, and installation, attractive appearance, ready availability, and high recyclability. However, significant copper-containing waste streams are produced from these industries.[1] Copper(II) is known to be one of the most toxic heavy metals to living organisms and it is one of the most widespread heavy metal contaminants of the environment.[2]

Current methods for the removal and recovery of copper(II) from its waste streams include precipitation, coagulation, filtration, adsorption, ion exchange, and electrochemical processes.[3] Adsorption is now recognized as an effective, efficient, and economic method for water decontamination applications and for analytical separation purposes.[4] Currently, there is an increasing emphasis on adsorbents based on naturally occurring support materials. Natural support materials possess a number of advantages, including the fact that they are available in large quantities, are relative cheap, and most importantly, can be chemically modified for enhanced metal binding ability. Some of these natural materials include chitosan,[5–7] zeolites,[8,9] clays,[10] and cellulose[11]; for example, chitosan's adsorptive capacity for some heavy metal ions was greatly increased by chemical modification.[3]

This work focuses on the use of cellulose as a naturally occurring polymeric base material in the preparation of a new adsorbent material for heavy metal contaminants. Cellulose is cheap, biodegradable, renewable, and the most abundant natural polymer in the world. The properties of cellulose may be modified by changing both the physical and chemical structure. The graft polymerization method has gained importance in modifying the chemical and physical properties of pure cellulose for different uses.[12,13] Adsorption of heavy metal ions is one application which has been studied in detail.[14–16] In this study, a two stage reaction scheme was conducted (Fig. 1). Initially,

Correspondence to: T. O'Dwyer; (tom.odwyer@ul.ie).
Contract grant sponsor: Materials & Surface Science Institute, University of Limerick, Ireland.
Contract grant sponsor: Enterprise Ireland.

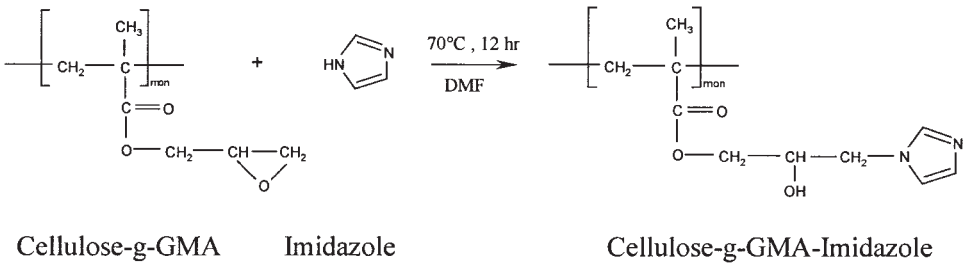

Figure 1 Reaction of Cellulose-*g*-GMA with Imidazole.

glycidyl methacrylate (GMA) was grafted onto regenerated cellulose fibers using ceric ammonium nitrate as initiator. Ceric ammonium nitrate (CAN) generates free radicals on the surface of the cellulose fibers which initiate the polymerization of GMA forming poly(GMA) chains off the surface of the fiber. The presence of GMA subsequently leaves the grafted product with a number of highly reactive epoxy groups that can be utilized in the second stage of the reaction scheme for the introduction of metal-specific functional groups into the grafted polymeric material. The cellulose-*g*-GMA was subsequently reacted with imidazole to add a metal binding ligand. While the metal binding ability of the imidazole ligand has been studied previously,[17,18] this research work was aimed to study the combined effects of naturally occurring support, grafting agent, and binding ligand.

EXPERIMENTAL

Materials

The regenerated cellulose (Chemcell™) was obtained from Borregaard Industries, Sarpsborg, Norway. Ceric ammonium nitrate (CAN), glycidyl methacrylate (GMA), imidazole, methanol, and acetone (technical grade) were provided by Sigma Aldrich, UK. The solvents were all of technical grade. The GMA was distilled to remove stabilizers before use. All aqueous solutions and standards were prepared using deionized water.

Adsorbent synthesis

Regenerated cellulose (0.5 g) was broken up into its fibrous form and placed in a glass grafting apparatus (Fig. 2) along with 30 mL of deionized water. The grafting reaction was carried out under nitrogen. The mixture of cellulose and 30 mL of water was bubbled with nitrogen for 10 min to remove traces of air trapped in the fibrous cellulose. The reaction temperature was controlled at 30°C. CAN (0.05*M*) and 10 mL of 0.1*M* nitric acid were added and allowed to react with the cellulose for 15 min. The excess initiator solution was removed by suction, and the cellulose fibers were rinsed with 100 mL of water. Fresh deionized water (40 mL) was charged into the glass grafting apparatus and bubbled with nitrogen for 5 min. GMA (0.35*M*) was then added and left to react for a further 2 h at 30°C under nitrogen. (Separately, 2–3 drops of pluronic nonionic surfactant was added to the GMA to keep it in an emulsified state.) The mixture was stirred. On completion of the reaction, the Cell-*g*-GMA product was removed and soxhlet extracted with acetone for 12 h to remove any GMA homopolymer. The Cell-*g*-GMA was then dried at 60°C under vacuum.[1,2] The cellulose-*g*-GMA was then ground up into free fibers and passed through a 500-μm sieve. The graft

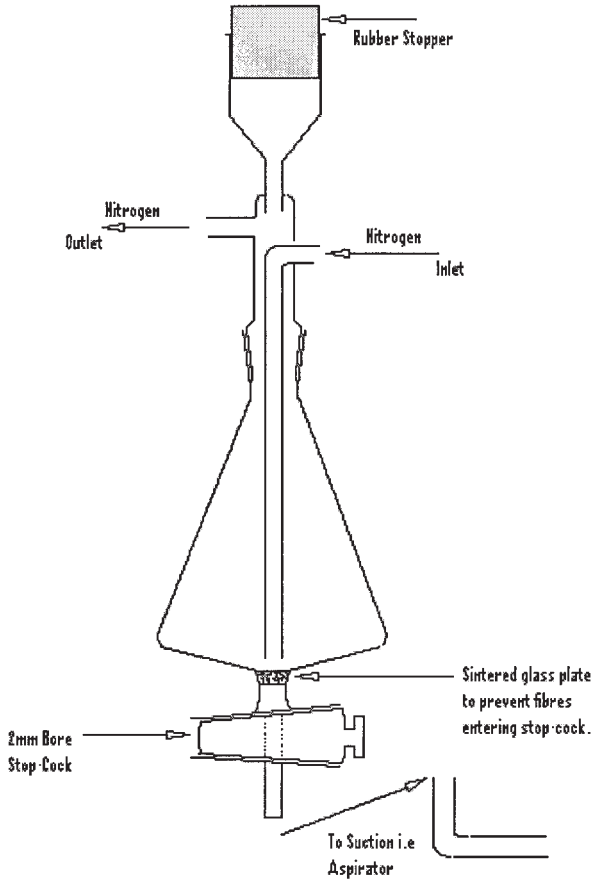

Figure 2 Grafting apparatus.

percentage was determined by the percent increase in weight as follows:

$$\% \text{ graft} = \frac{W_g - W_0}{W_0} \times 100 \quad (1)$$

where W_0 and W_g represent the weights of the initial and the grafted fiber, respectively.

Imidazole (3.0 g) was reacted with the cellulose-*g*-GMA fibers (3.0 g) in 120 mL dimethyl formamide solution at 70°C for given durations. The cellulose-*g*-GMA-imidazole material was then filtered and rinsed with water and soxhlet extracted with methanol for 6 h to remove any unreacted imidazole residue. The adsorbent was then dried in a vacuum oven at 70°C under vacuum, ground up with a mortar and pestle, and passed through a 300-μm sieve.

Adsorption experiments

Adsorption isotherms

A series of copper(II) solutions of various initial concentrations (25–6000 ppm) were prepared by dissolving appropriate amounts copper(II)sulfate, $CuSO_4.5H_2O$ (Merck, Germany), in deionized water. From each flask, a 25-mL aliquot was removed and placed in a separate 50-mL plastic vial and 0.2 g of the adsorbent, cellulose-*g*-GMA-imidazole, was added to each vial. Each vial was then sealed and attached to a flask shaker (Gallenkamp, UK) and shaken for 2 h. After 2 h, the vials were centrifuged using a Rotofix 32 centrifuge (Hettich Zentrifugen) at 6000 rpm for 15 min. An aliquot of each supernatant was then removed and suitably diluted with deionized water and analyzed by atomic absorption spectrophotometry (AAS) (Varian SpectraAA 220). Blank solutions containing equivalent initial concentrations of copper but without addition of the sorbent (cellulose-*g*-GMA-imidazole) were prepared and put through the identical procedures. Standard copper AAS solutions were prepared in the range 1–10 ppm using a 1000 ppm AAS stock solution (Reagecon Diagnostics). Adsorption isotherms were carried out at 7, 23, and 40°C. All samples and blanks were run in triplicate to ensure reproducibility and accuracy.

Kinetics studies

Adsorption kinetics for copper (II) uptake on cellulose-*g*-GMA-imidazole were studied using the batch technique. The investigations were conducted at 23°C by monitoring the decrease in the copper (II) solution concentration with time. Known weights of cellulose-*g*-GMA-imidazole (0.2 g) were added to each vial containing 25 mL of the copper (II) solution. Initial copper (II) solution concentrations were 100, 300, and 600 ppm. The vials were shaken in a temperature-controlled water bath shaker for various time periods and subsequently centrifuged. The concentration of copper (II) before and after adsorption was determined by AAS. The amount adsorbed was calculated from the initial and final concentrations of copper (II) in the aqueous phase. All samples and blanks were run in triplicate to ensure reproducibility and accuracy.

Characterization

Analytical methods

Fourier transform infrared spectroscopy: Fourier transform infrared spectroscopy (FTIR) of the unmodified regenerated cellulose, cellulose-g-GMA, and cellulose-g-GMA-imidazole were recorded using a PerkinElmer Spectrum 2000 instrument. A weight of sample (2 mg) was mixed with 100 mg of FTIR-grade KBr. The samples were scanned 30 times at 4 cm^{-1} resolution in the 4000–400 cm^{-1} range and then averaged.

Scanning electron microscopy: Scanning electron micrographs of the unmodified cellulose pulp fiber, cellulose-*g*-GMA, and cellulose-*g*-GMA-imidazole were taken using a Jeol JSM 840 scanning electron microscope. The samples were sputter coated in gold using an Edward sputter coater.

Thermogravimetric and differential thermal analysis: Thermogravimetric analysis (TGA) and the differential thermal analysis (DTA) were done using a Stanton Redcroft DTA/TGA 1600 (Rheometric Scientific, Epson, UK). The TGA and DTA curves were produced up to 600°C, starting at 95°C, at a heating rate of 10°C min^{-1}, under a nitrogen atmosphere. Alumina was used as reference material.

Determination of the epoxy group content: The available epoxy group content of the cellulose-*g*-GMA was determined by the HCl-dioxane method of titration.[19] This method consists of reacting HCl with epoxy groups in an appropriate organic solvent. Chlorohydrin is produced as a result of the acid opening the epoxy groups.

Elemental analysis: The degree of epoxide and amine substitution in the cellulose was analyzed by elemental analysis data. Analysis was carried out at the Microanalytical Laboratory, UCD, Dublin, Ireland.

pH studies: All pH studies were carried out using a Jenway 3015 digital pH meter. Buffer solutions (pH 4, 7, and 11) (Merck) were used to calibrate the instrument. Copper (II) adsorption solution concentrations were altered using 0.1M HCl and NaOH solutions.

RESULTS AND DISCUSSION

FTIR characterization of the fibrous adsorbent

The FTIR spectra of the ungrafted cellulose wood pulp, cellulose-*g*-GMA, and cellulose-*g*-GMA-imida-

zole are presented in Figure 3. Characteristic absorption peaks for poly(GMA) occur at 1720 cm^{-1}(carbonyl group) and 985, 901, and 838 cm^{-1} (epoxy group) in the grafted fiber.[20] These adsorption peaks are also visible in cellulose-*g*-GMA, providing evidence that grafting of GMA to the cellulose surface had occurred. The FTIR spectrum of cellulose-*g*-GMA-imidazole in Figure 3 shows ligand peaks at 3000–3500 cm^{-1} (very broad, im-NH and/or CH_2—NH—CH_2 stretching vibrations) and in Figure 4 at 1570 cm^{-1} (imidazole ring vibration). The epoxy group peaks appearing in cellulose-*g*-GMA at 840, 902 cm^{-1} (epoxy vibrations), and 1340 cm^{-1} [δ(CH) epoxy] disappear completely, indicating reaction of the epoxy groups on the cellulose-*g*-GMA with the imidazole ligand. Also, additional peaks can be seen on cellulose-*g*-GMA-imidazole in Figure 4, at 1513cm^{-1} (C—C/N—C stretching), 1235cm^{-1} (ring vibration), and 1106cm^{-1} (in plane ring C—H bending), giving more evidence of the functionalization reaction with imidazole.[21]

SEM characterization

Scanning electron micrographs were used to examine the surface morphology of the cellulose fibers and the cellulose-*g*-GMA intermediate. To clarify the changes in morphology due to the grafting of GMA, micrographs of the investigated samples are presented with two different instrument magnifications [Figs. 5(a) and 5(b)]. The results show a pronounced swelling effect on the fiber and the surface of the grafted fibers look rougher. The diameter of individual fibers seems to become thicker on the grafted cellulose.

TGA and DTA characterization

TGA and DTA curves of cellulose wood pulp, cellulose-*g*-GMA, and cellulose-*g*-GMA-imidazole are presented in Figures 6 and 7. The differences in thermal behavior for all three samples of cellulose are reflected in (1) the temperatures corresponding to the onset of weight loss, (2) the rate of weight loss, (3) the magnitude of the enthalpy change, and (4) the values of the peak temperature of the DTA curve.[22] Figures 6 and 7 show the simultaneous TGA/DTA plots for the cellulose pulp, cellulose-*g*-GMA, and cellulose-*g*-GMA-imidazole. Analysis commenced at 100°C. Four distinct regions can be distinguished by examining the DTA curve for cellulose wood pulp in the temperature region below 365°C. An initial endothermic peak occurs at 130°C and is attributed to removal of the water of hydration in the sample. Two small endothermic peaks occur at 275 and 320°C and are concurrent with a slow weight loss, due to dehydration and depolymerization-tar-forming processes. There is a slight exothermic peak between these two endothermic peaks and this is believed to be the product of the endothermic processes.[23] From 240 to 370°C is attributed to the thermal cleavage of the glycosyl units and scission of other C—O bonds via a free radical reaction.[24] From Figure 7, it can be seen that cellulose-*g*-GMA samples show an additional endothermic peak, representing degradation of poly(GMA) at 390°C. The exothermic peak at 350°C is due to some reaction (or reactions) of the epoxy group. It has been reported that in poly(GMA), the first degradation occurs at 360°C, with complete degradation at 435°C.[25] The first endothermic peak, which occurs at 250°C, may be due to the decomposition of the grafted epoxide groups.[26] The DTA curve for cellulose-*g*-GMA-imidazole shows an additional deep endothermic peak at 435°C due perhaps to the decomposition of the imidazole ligand. In poly(vinyl imidazole) endothermic peaks occur at 320 and 460°C and may be due to the degradation of protonated and unprotonated imidazole rings respectively.[27] From the TGA curves, it can be seen that the starting temperature of thermal degradation of the cellulose samples becomes lower, indicating loss in

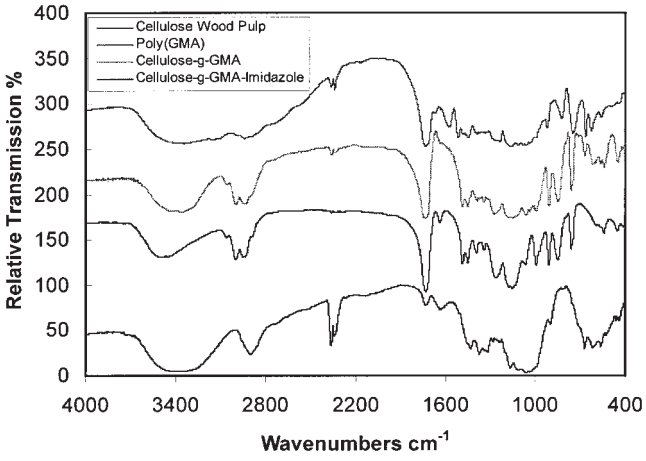

Figure 3 FTIR spectra of cellulose, poly(GMA), cellulose-*g*-GMA, and cellulose-*g*-GMA-Imidazole.

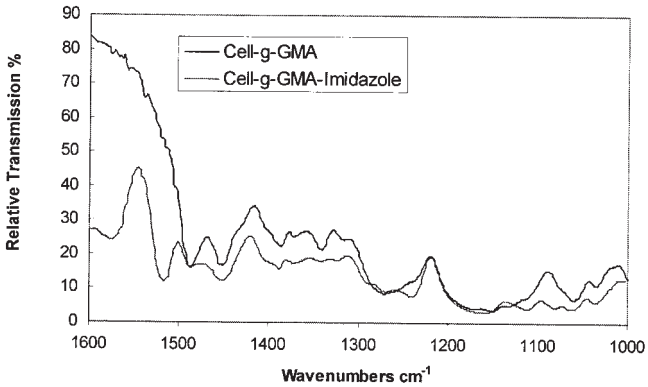

Figure 4 FTIR spectra of cellulose-*g*-GMA and cellulose-*g*-GMA-imidazole in the 1600–1000 cm^{-1} range.

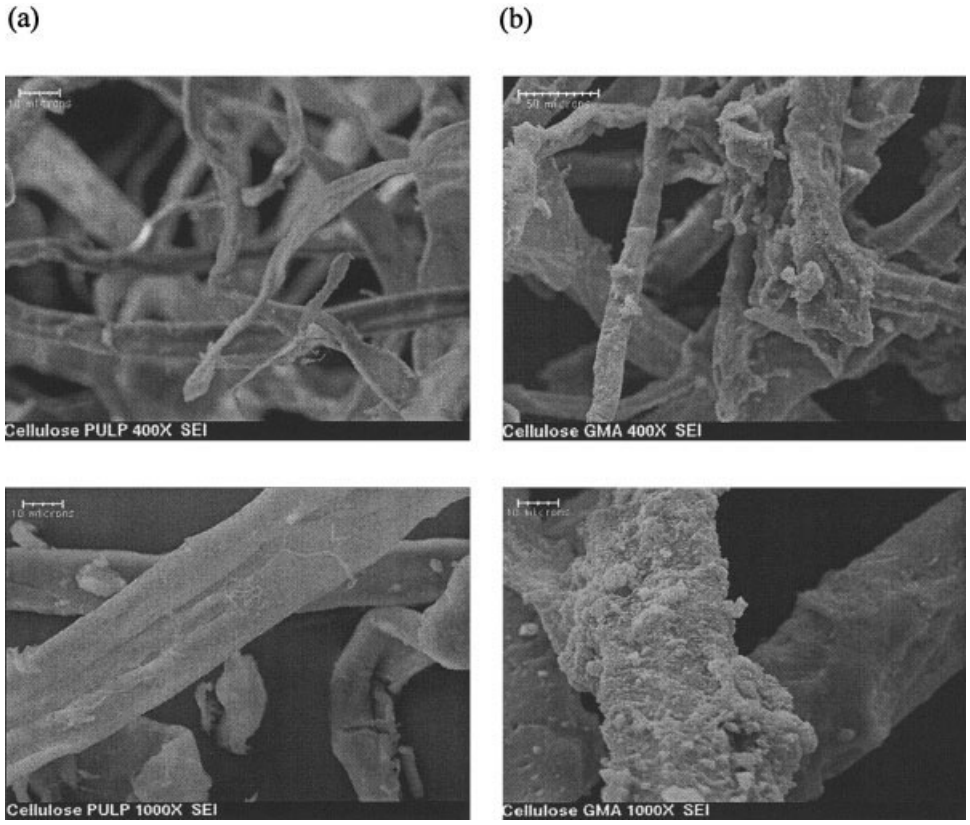

Figure 5 Surface morphology of (a) ungrafted and (b) grafted cellulose pulp with GMA. (a) Magnification 400×; (b) magnification 1000×.

thermal stability on grafting and a slight increase in thermal stability on functionalization of the cell-*g*-GMA fibers. The DTA curves would indicate an increase in thermal stability with functionalization of cellulose-*g*-GMA with imidazole, as can be seen from the endothermic peak shifting from 250°C in cellulose-*g*-GMA to 290°C in cellulose-*g*-GMA-imidazole. This may suggest that an increase in the nitrogen content of cellulose led to an increase in the decomposition temperature of cellulose derivatives.

Determination of the epoxy groups content

A derivative procedure of the HCl-dioxane method described by Kling and Ploehn[19] was used in this study to determine the amount of free epoxy groups on the cellulose-*g*-GMA intermediate material. The

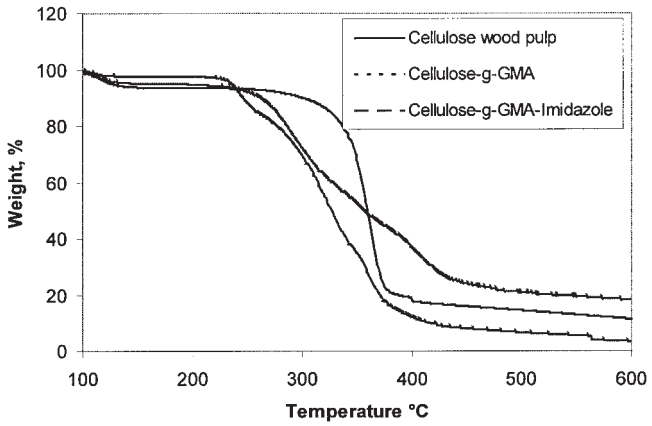

Figure 6 TGA curves for cellulose wood pulp, cellulose-*g*-GMA, and cellulose-*g*-GMA-imidazole.

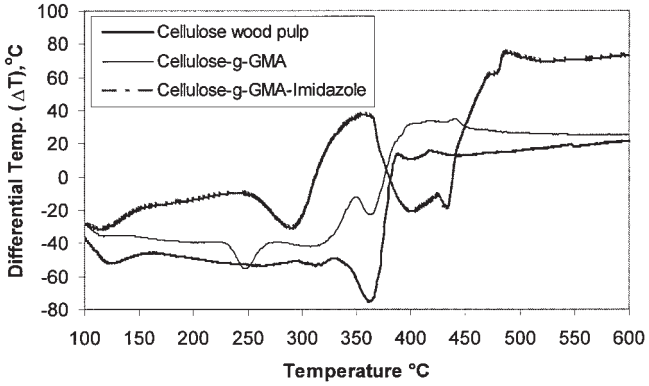

Figure 7 DTA curves for cellulose wood pulp, cellulose-*g*-GMA, and cellulose-*g*-GMA-imidazole.

TABLE I
Elemental Analysis of Cellulose, Cellulose-*g*-GMA, and Cellulose-*g*-GMA-Imidazole

Sample	% C	% H	% N
Cellulose wood pulp	41.63	6.07	0.0
Cellulose-*g*-GMA	52.22	6.63	0.0
Cellulose-*g*-GMA-imidazole	50.49	6.46	8.09

method involves, initially, reacting a defined amount of HCl with cellulose-*g*-GMA to open free epoxy rings, and the residual HCl is backtitrated with NaOH. The exact amount of free epoxy groups can thus be calculated from the amount of HCl consumed. In this study, the cellulose-*g*-GMA intermediate material was examined and found to contain 1.75 mmol g^{-1} free epoxy groups.

Elemental analysis characterization

Table I outlines the results of the elemental analysis carried out on the cellulose wood pulp, cellulose-*g*-GMA, and cellulose-*g*-GMA-imidazole. Elemental analysis indicates an increase in relative carbon and hydrogen compositions following the grafting procedure. The presence of nitrogen in the cellulose-*g*-GMA-imidazole product alone provides further evidence of the functionalization of the cellulose-*g*-GMA intermediate product.

Adsorption

An adsorption isotherm can be used to characterize the interaction of metal ions with adsorbents. The isotherm provides a relationship between the concentration of metal ions in solution and the amount of metal ions adsorbed on to the solid phase when both phases are at equilibrium.[18] The adsorption isotherms for Cu(II) on cellulose-*g*-GMA-imidazole at different temperatures are shown in Figure 8. Preliminary tests on equilibrium time for Cu(II) adsorption on cellulose-*g*-GMA-imidazole revealed significant uptake within the first 15–20 min, and full adsorption occurred after 30 min.

Adsorption levels were similar for all three temperatures. At 7°C, copper adsorption on cellulose-*g*-GMA-imidazole reached a level of 65.62 mg g^{-1}, 68.75 mg g^{-1} at 23°C, and 62.5 mg g^{-1} at 40°C.

The adsorption isotherm data were analyzed by both the Langmuir and Freundlich models, as defined in eqs. (2) and (3).[28,29]

$$q_e = \frac{K_L C_e}{1 + A_L C_e} \tag{2}$$

$$q_e = K_F C_e^{1/n} \tag{3}$$

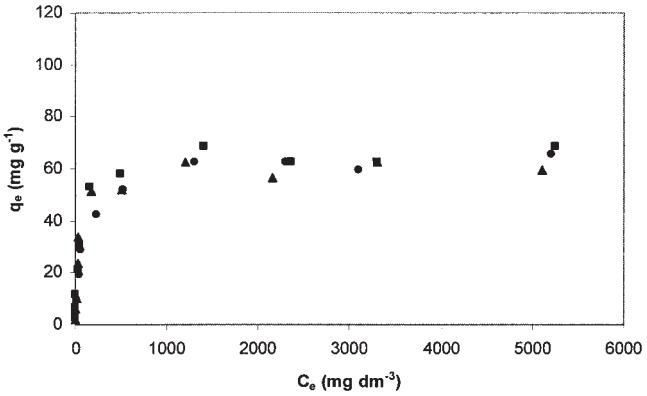

Figure 8 Adsorption isotherms for Cu(II) on cellulose-*g*-GMA-imidazole at 7°C (♦), 23°C ■, and 40°C (▲).

where q_e is the amount of solute adsorbed at equilibrium per gram of adsorbent, C_e is equilibrium concentration in solution in milligram per decimeter, and K_L and A_L are Langmuir constants. A plot of C_e/q_e versus C_e from the linear form of eq. (2) was used to determine the values of K_L (intercept) and A_L/K_L (slope). Saturation coverage on the adsorbent was obtained as $K_L/A_{L.}$

The Freundlich isotherm model is entirely an empirical isotherm and assumes a logarithmic relationship between the level of adsorption and equilibrium sorbate concentration and can be represented by the linearized form of eq. (3).

$$\ln q_e = \ln K_F + \frac{1}{n} \ln C_e \tag{4}$$

where K_F and n are Freundlich constants related to adsorption capacity and energy of adsorption, respectively.[30] The adsorption data were fitted to the Langmuir and Freundlich Isotherm models, and Figure 9 shows the Langmuir plot.

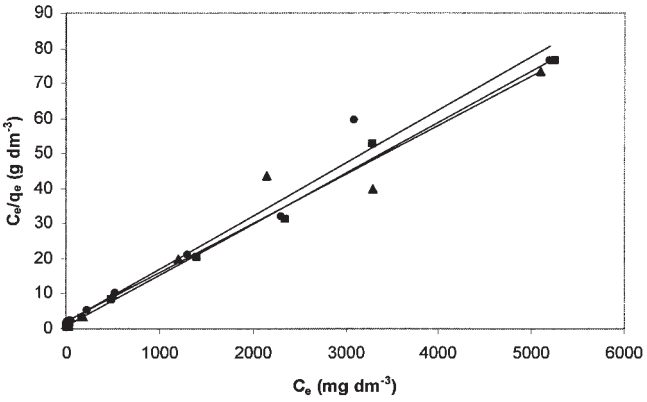

Figure 9 Langmuir isotherms for Cu(II) adsorption on cellulose-*g*-GMA-imidazole at 7°C (♦), 23°C (■), and 40°C (▲).

TABLE II
Langmuir and Freundlich Constants for Cu(II) Adsorption on Cellulose-*g*-GMA-Imidazole

Temperature (°C)	K_L ($dm^3\ g^{-1}$)	K_F ($dm^3\ g^{-1}$)	A_L ($dm^3 m\ g^{-1}$)	K_L/A_L ($mg\ g^{-1}$)	n	R^2
Langmuir isotherm data						
7	0.5879		0.00893	65.79		0.9757
23	1.5508		0.02264	68.49		0.9947
40	0.4832		0.00676	71.43		0.9607
Freundlich isotherm data						
7		5.294			3.059	0.9172
23		9.870			3.924	0.8188
40		9.870			3.924	0.8188

The Langmuir model yielded high correlation coefficient values (R^2) of 0.976 for 7°C, 0.961 for 40°C, and 0.995 for 23°C. The Langmuir constants were calculated using eq. (2) and are shown in Table II. K_L/A_L is used to estimate the monolayer or saturation coverage of Cu(II) on the adsorbent. It was calculated as 65.79 mg g^{-1} for 7°C, 68.49 mg g^{-1} for 23°C, and 71.43 mg g^{-1} for 40°C.

Modeling the data to the Freundlich model yielded significantly lower correlation coefficients, as outlined in Table II.

Influence of pH

The removal of pollutants from wastewaters by adsorption is highly dependent on sorbate solution pH. Variation of pH can affect the surface charge of the adsorbent, and the degree of ionization and speciation of adsorbate.[31] The effect of initial solution pH on copper sorption onto cellulose-*g*-GMA-imidazole was studied at room temperature by varying the pH between 2.0 and 7.0 (Fig. 10). It can be seen that the sorption of copper increases as the pH increases, from a low value of 13.26% at pH 2.0 to its maximum of 97.33% at pH 7.0. The influence of pH on the removal of Cu(II) can be explained on the basis of the electrostatic interaction model.[32] As the pH decreases, the surface of the cellulose-*g*-GMA-imidazole exhibits an increasingly positive characteristic. The species to be adsorbed, Cu^{2+}, is positively charged, and at very low pH values, the adsorption is not favored. Effectively, competition between H^+ ions present and Cu^{2+} ions minimizes the extent of copper adsorption. As the pH increases, the adsorbent surface becomes more negatively charged and therefore the adsorption of positively charged Cu^{2+} and $Cu(OH)^+$ species is more favorable.[33] As the pH of the solution increases above 5, Cu^{2+} removal by precipitation as $Cu(OH)_2$ starts to occur. The very high perceived uptake of Copper(II) above pH 5 is mainly due to this precipitation of $Cu(OH)_2$ and not the adsorption capability of cellulose-*g*-GMA-imidazole.

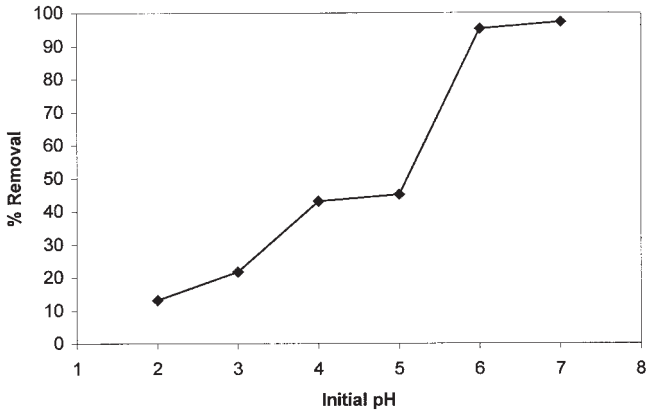

Figure 10 Removal of Cu(II) by cellulose-*g*-GMA-imidazole, as a function of pH. Conditions: 1000 ppm $CuSO_4$ solution; Temperature, 23°C; cellulose-*g*-GMA-imidazole, 0.2 g; Time, 1 h.

Thermodynamics

To explain the effect of temperature on the adsorption processes, the thermodynamic parameters of standard free energy (ΔG^0), standard enthalpy (ΔH^0), and standard entropy (ΔS^0) were determined.[34]

These thermodynamic parameters for the adsorption of copper were calculated by using eqs. (5)–(8), and the values of the thermodynamic parameters are outlined in Table III.

$$K_C = \frac{q_e}{C_e} \tag{5}$$

TABLE III
Thermodynamic Parameters for the Adsorption of Cu(II) on Cellulose-*g*-GMA-Imidazole

−ΔG° (KJ mol^{-1})			ΔH°	ΔS°
7°C	23°C	40°C	(kJ mol^{-1})	(J k^{-1} mol^{-1})
8.50	11.47	9.22	−2.70	24.11 ± 4.81

$$\Delta G^0 = -RT \ln K_C \quad (6)$$

$$\Delta H^0 = -R\left[\frac{T_2 \times T_1}{(T_2 - T_1)}\right] \ln \frac{k_{c2}}{k_{c1}} \quad (7)$$

$$\Delta S^0 = -\frac{(\Delta G^0 - \Delta H^0)}{T} \quad (8)$$

where k_{C1}, $k_{C2,}$ and k_{C3} are equilibrium constants at temperatures $T_{1,}$ $T_{2,}$ and $T_{3,}$ respectively, obtained from the Langmuir isotherms,[35] q_e is the amount of solute (mol) adsorbed on the adsorbents (cubic decimeter of the solution at equilibrium), and C_e is the equilibrium concentration (mol dm^{-3}) of the solute in solution. T is the temperature in Kelvin and R is the gas constant.[36].

The negative values of the Gibbs free energy (ΔG^0) at various temperatures indicate the spontaneous nature of the adsorption and the feasibility of the process. The increase in ΔG^0 from 7 to 23°C shows that the adsorption is more favorable at high temperatures.[24] The positive value of enthalpy (ΔH^0) indicates that the adsorption is endothermic, and the positive value of entropy change (ΔS^0) reflects an affinity of cellulose-*g*-GMA-imidazole for the Cu(II) adsorbate,[37] and suggests some structural changes in copper and the adsorbent.[38]

Kinetic parameters

To apply the adsorption technique to larger scale processes, the elucidation of the kinetic parameters and sorption characteristics of the adsorbent material is necessary. The two primary issues to be addressed are contact time for equilibrium adsorption and the influence of initial adsorbate concentration on uptake. The influence of initial concentration on the rate of Cu(II) uptake can be seen in Figure 11.

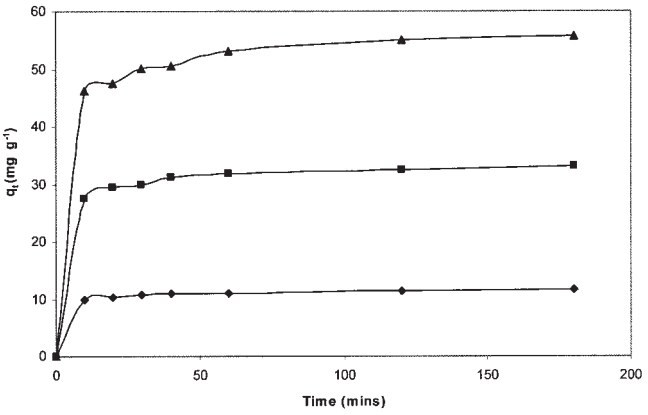

Figure 11 Kinetics of Cu(II) uptake by cellulose-*g*-GMA-imidazole at 100 mg dm^{-3} (♦), 300 mg dm^{-3} (■), and 600 mg dm^{-3} (▲).

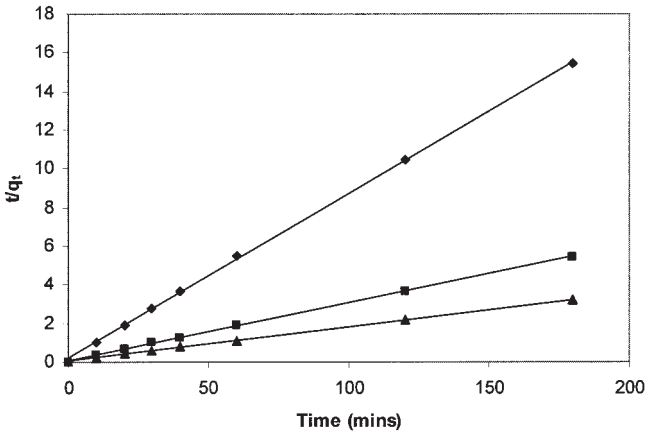

Figure 12 Second-order sorption kinetics of Cu(II) on cellulose-*g*-GMA-imidazole at concentrations of 100 mg dm^{-3} (♦), 300 mg dm^{-3} (■), and 600 mg dm^{-3} (▲).

Preliminary adsorption tests on the rate of Cu(II) uptake by cellulose-*g*-GMA-imidazole indicated that the adsorption process is quite rapid, with maximum adsorption and equilibrium conditions being reached within 15–30 min.

Two rate equations were used to analyze the adsorption kinetics data—pseudo-first- and second-order reaction kinetics. The results are presented in Figure 12 and Table IV.

Lagergren's pseudo-first-order kinetic expression eq. (9) can be represented in linear form eq. (10).

$$\frac{dq_t}{dt} = k_1(q_e - q_t) \quad (9)$$

$$\ln (q_e - q_t) = \ln q_e - k_1 t \quad (10)$$

The term k_1 refers to the pseudo-first-order rate constant for the sorption process (per minute). Parameters derived from the pseudo-first-order plots or the Cu(II) adsorption data are shown in Table IV.

Pseudo-second-order kinetics [eq. (11)] can be used to assess the dependency of the process on the sorbed Cu(II) concentration.[39]

$$\frac{dq_t}{dt} = k_2(q_e - q_t)^2 \quad (11)$$

where k_2 is the overall rate constant for the adsorption process [dm^3 (mg min^{-1})], q_e is the amount of Cu(II) adsorbed at equilibrium (mg g^{-1}), and q_t is the amount of Cu(II) adsorbed at any time t (mg g^{-1}). Rearrangement of eq. (11) leads to the linearized form, as outlined in eq. (12).

$$\frac{t}{q_t} = \frac{1}{k_2 q_e^2} + \frac{1}{q_e} t \quad (12)$$

TABLE IV
Effect of Initial Cu(II) Concentration on Sorption Data on Cellulose-*g*-GMA-Imidazole Using the Pseudo-Second-Order and Pseudo-First-Order Approaches

Initial Cu(II) concentration (mg dm^{-3})	Correlation coefficient (R^2)	Equilibrium Cu(II) uptake (mg g^{-1})	Rate constant, k_1 (g mg^{-1} min^{-1})	Rate constant, K_2 (g mg^{-1} min^{-1})	Initial sorption rate, h (mg g^{-1} min^{-1})
Pseudo-second-order kinetic parameters					
100	0.9995	11.68	3.59×10^{-2}		4.90
300	0.9997	33.12	1.36×10^{-2}		14.99
600	0.9995	55.62	6.54×10^{-3}		20.24
Pseudo-first-order kinetic parameters					
100	0.7121	3.25		2.45×10^{-2}	
300	0.7319	9.258		2.69×10^{-2}	
600	0.8598	19.77		3.13×10^{-2}	

The initial sorption rate, h, as $t \rightarrow 0$ can be defined as

$$h = k_2 q_e^2 \tag{13}$$

The initial sorption rate, h, the equilibrium sorption capacity, q_e, and the pseudo-second-order rate constant, k_2, can be determined experimentally from slope and intercept by plotting t/q_t against t.[38]

Analysis of both pseudo-first- and second-order plots and the resulting parameters (Fig. 12 and Table IV) clearly indicates that the kinetics of Cu(II) adsorption on cellulose-*g*-GMA-imidazole strongly correlates with the pseudo-second-order kinetic process.

All plots show very high correlation coefficients (R^2) and good conformity with the proposed pseudo-second-order equation. The initial sorption rates (h values) increased with an increase in initial copper ion concentration. The data show an increase in Cu(II) uptake capacity for higher initial Cu(II) concentrations and that the initial Cu(II) concentration influences the contact time necessary to reach equilibrium. The values of the overall sorption rate constants, k_2, were found to increase substantially with increasing initial concentration from 100 to 300 mg dm^{-3} and to decrease from 300 to 600 mg dm^{-3}. Correlation coefficients (R^2) for the pseudo-first-order equations are lower than the comparable pseudo-second-order equation coefficients. This indicates strictly that the sorption of Cu(II) by cellulose-*g*-GMA-imidazole is more accurately represented by the pseudo-second-order kinetics process.

CONCLUSIONS

The graft copolymerization of the vinyl monomer glycidyl methacrylate (GMA) on regenerated cellulose wood pulp and the subsequent functionalization of this grafted polymer with imidazole were carried out and characterized. Spectroscopic (FTIR) and titrometric evidence suggest that imidazole successfully functionalized the cellulose-*g*-GMA. As a further evaluation of cellulose-*g*-GMA-imidazole material, adsorption tests were carried out to investigate the material's ability to remove Cu^{2+} from aqueous solution. The adsorption isotherm indicated clearly that the reaction product has an adsorptive capacity and was capable of removing 68.49 mg Cu^{2+} g^{-1} of reaction product. This adsorption follows a Type I process and fits the assumptions of the Langmuir isotherm. Kinetics data on the adsorbent determined that the Cu(II) uptake was very rapid, with maximum uptake occurring at approximately the 20-min mark. These tests also demonstrated the dependence of the adsorption process on the initial concentration of Cu(II) in solution, with uptake rising with increased concentration. Further examination revealed a correlation of the process to the pseudo-second-order kinetics model. It was notable, however, that the overall rate constants and the initial sorption rates decreased as a result of higher initial concentrations of Cu(II). The adsorption process was shown not to be affected significantly by temperature and the ideal pH of adsorption was shown to be pH 4.5. These findings suggest that cellulose-*g*-GMA-imidazole exhibits significant potential as an adsorbent in the removal of heavy metals from industrial wastewaters.

References

1. Lee, C. I.; Yang, W. F.; Hsieh, C.-I. Chemosphere 2004, 57, 1173.
2. Ozer, A.; Ozer, D.; Ozer, A. Process Biochem 2004, 39, 2183.
3. Li, N.; Bai, R. Sep Purif Technol 2005, 42, 237.
4. Crini, G. Prog Polym Sci 2005, 30, 38.
5. Guibal, E. Sep Purif Technol 2004, 38, 43.
6. Chu, K. H. J Hazard Mater 2002, 90, 77.
7. Wan Ngah, W. S.; Endud, C. S.; Mayanar, R. React Funct Polym 2002, 50, 181.
8. Erdem, E.; Karapinar, N.; Donat, R. J Colloid Interface Sci 2004, 280, 309.
9. Ouki, S. K.; Kavannagh, M. Water Sci Technol 1999, 39, 115.
10. Naseem, R.; Tahir, S. S. Water Res 2001, 35, 3982.
11. Bicak, N.; Sherrington, D. C.; Senkal, B. F. React Funct Polym 1999, 41, 69.

12. Gurdag, G.; Yasar, M.; Gurkaynak, M. J Appl Polym Sci 1997, 66, 929.
13. Vitta, S. B. J Macromol Sci Chem 1985, A22, 579.
14. Iwakura, Y.; Kurosaki, T.; Uno, K.; Imai, Y. J Polym Sci Part C: Polym Symp 1964, 4, 673.
15. Kubota, H.; Suzuki, S. Eur Polym J 1995, 31, 701.
16. Waly, A.; Abdel-Mohdy, F. A.; Hebeish, A. J Appl Polym Sci 1998, 68, 2151.
17. Van Berkel, P. M.; Dreissen, W. L.; Reedijk, J.; Sherrington, D. C.; Zitsmanis, A. React Funct Polym 1995, 27, 15.
18. Kara, A.; Uzun, L.; Nand, B.; Denizli, A. J Hazard Mater 2004, 106, 93.
19. Kling, J. A.; Ploehn, H. J Polym Sci Part A: Polym Chem 1995, 33, 1107.
20. Navarro, R. R.; Sumi, K.; Matsumura, M. Water Res 1999, 33 2037.
21. Wu, K. H.; Chang, T. C.; Wang, Y. T.; Hong, Y. S.; Wu, T. S. Eur Polym J 2003, 39, 239.
22. Yang, P.; Kokot, S. J Appl Polym Sci 1996, 60, 1137.
23. Conley, R. T. Thermal Stability of Polymers, Vol. 1; Marcel Dekker: New York, 1970.
24. Huang, M. R.; Li, X. G. J Appl Polym Sci 1998, 68, 293.
25. Shukla, S. R.; Athalye, A. R. J Appl Polym Sci 1995, 57, 983.
26. Li, H.; Wang, L.; Jacob, K.; Wong, C. P. J Polym Sci Part A: Polym Chem 2002, 40, 1796.
27. Pekel, N.; Guven, O. Polym Int 2002, 51, 1401.
28. Langmuir, I. J Am Chem Soc 1918, 40, 1361.
29. Freundlich, H. J Phys Chem 1926, 7, 57.
30. Ortiz, N.; Pires, M. A. F.; Bressiani, J. C. Waste Manag 2001, 21, 631.
31. Elliott, H. A.; Huang, C. P. Water Res 1981, 15, 849.
32. Bhattacharya, K.; Venkobacher, C. J Environ Eng Div ASCE 1984, 110, 110.
33. Periasamy, K.; Namasiuayam, C. Chemosphere 1996, 32, 769.
34. Bereket, G.; Aroguz, A. Z.; Ozel, M. Z. J Colloid Interface Sci 1997, 187, 338.
35. Gupta, V. K.; Jain, C. K.; Ali, I.; Sharma, M.; Saini, V. K. Water Res 2003, 37, 4038.
36. Romero-Gonzalez, J.; Peralta-Videa, J. R.; Rodríguez, E.; Ramirez, S. L.; Gardea-Torresdey, J. L. J Chem Thermodyn 2005, 37, 343.
37. Kelleher, B. P.; O'Callaghan, M. N.; Leahy, M. J.; O'Dwyer, T. F.; Leahy, J. J. J Chem Technol Biotechnol 2002, 77, 1212.
38. Ho, Y. S. Water Res 2003, 37, 2323.
39. Xing, B.; McGill, W. B.; Dubas, M. J Environ Sci Technol 1994, 28, 466.